Turkish J. Eng. Env. Sci.
31 (2007) , 273 – 288.

Plane Strain Analytical Solutions to Rotating Partially Plastic Graded Hollow Shafts

Ahmet N. ERASLAN and Eray ARSLAN
Department of Engineering Sciences Middle East Technical University, 06531, Ankara-TURKEY
e-mail: aeraslan@metu.edu.tr

Received 06.03.2006

Abstract

Analytical solutions for the elastoplastic deformation of rotating graded hollow shafts are presented. The modulus of elasticity of the shaft material is assumed to vary nonlinearly in the radial direction. The plastic model is based on Tresca's yield criterion, its associated flow rule, and ideal plastic material behavior. Elastic, partially plastic, fully plastic, and residual stress states are investigated. It is observed that the elastoplastic responses of the rotating functionally graded hollow shafts are affected notably by the material nonhomogeneity. It is also observed that the fully plastic limit rotation speed of the shaft is almost independent of the variation in the modulus of elasticity of the material. The nonhomogeneous solution derived here reduces to that of a homogeneous one as the variation in the modulus of elasticity is slowed down.

Key words: Functionally graded material, Elastoplasticity, Rotating shafts, Stress analysis, Tresca's criterion

Introduction

Estimation of elastic, partially plastic, and residual stress states in rotating circular shafts is an important topic in engineering because of the many known rigorous applications. For this reason, a number of important studies pertaining to the elastic and partially plastic deformations of rotating homogeneous circular shafts were performed in the past under plane strain presupposition. Details of these investigations may be found in research articles Gamer and Lance (1983), Mack (1991a, 1991b, 1998), Gamer et al. (1997), Eraslan (2002, 2004), Eraslan and Mack (2005), and in the references cited therein. More recently, the stress response of rotating solid shafts made of functionally graded materials (FGMs) was studied analytically in the elastic stress state by Eraslan and Akis (2006), with emphasis on the onset of plastic deformation. However, a careful search of existing literature reveals that the partially plastic stresses and deformations in rotating FGM shafts have never been investigated in theory, although various authors have recognized the advantages of using FGM in operations (Horgan and Chan, 1999; Zimmerman and Lutz, 1999; Güven, 2001, Tutuncu and Ozturk, 2001; Liew et al., 2003; Eslami et al., 2005; Eraslan and Akis, 2006). This work aims to fill to some extent the gap in the literature in this respect.

The objective of this work is to derive a consistent analytical solution to describe elastic and partially plastic deformations of rotating FGM hollow shafts. An FGM is nonhomogeneous in composition and so its properties, especially those of modulus of elasticity, thermal conductivity, and mass density, may vary continuously throughout the material. Since the modulus of elasticity, E, is important in the determination of the strength of the structural element during operation, it is of engineering interest to ascertain the effect of variable modulus of elasticity on the deformation behavior of basic structures. In this work the modulus of elasticity of the shaft material is assumed to vary radially according to a power law

form given by (Horgan and Chan, 1999)

$$E(r) = E_0 \left(\frac{r}{b}\right)^n. \tag{1}$$

Here, E_0 is the reference value of E, b the outer radius, r the radial coordinate, and n a material parameter. With this form, a wide range of nonlinear and continuous profiles to describe reasonable variation in E in the material may be achieved.

The homogeneous counterpart of the problem under consideration has already been solved by Mack (1991a) for axially unconstrained ends. A sufficiently long rotating hollow shaft of inner radius a and outer radius b was taken into account. Assuming a perfectly plastic shaft material and using incremental theory of plasticity accompanied by Tresca's yield criterion, all stages of elastoplastic response of the homogeneous shaft were studied. It was demonstrated by Mack in his article that the inner surface of the elastic shaft is critical and the plastic deformation commences at this surface by a side regime in Tresca's hexagon as soon as the rotation speed is increased to the elastic limit. As this plastic region propagates toward the outer surface with increasing rotation speeds, another critical limit is reached at which the stress state moves to a corner regime. Thereafter, a corner regime and an adjacent side regime appear simultaneously, and hence the plastic core consists of 3 annular regions governed by different forms of Tresca's yield criterion. All 3 plastic regions expand with increasing rotation speeds until the homogeneous hollow shaft becomes fully plastic. The present work represents an extension of Mack's solution to shafts made of functionally graded materials. An elastic region as well as 3 plastic regions governed by different mathematical forms of Tresca's yield criterion are formulated for variable E and solved analytically. All stages of elastic-plastic deformation are studied and the complete solution is verified in comparison to Mack's by taking the limit as the material parameter n gets smaller. It should be noted at this point that, depending on how E varies in the shaft, even the rotating FGM solid shaft may undergo plastic deformation in a manner entirely different from that of its homogeneous counterpart (Eraslan and Akis, 2006). Therefore, the extremities of the material parameter n as well as the aspect ratio a/b that possibly lead to different partially plastic responses of the rotating FGM hollow shaft are not dealth with in the present work.

On the other hand, the solution of rotating hollow shaft with axially constrained ends can be obtained as the subset of the present solution by letting the deformation in the axial direction vanish. This problem is also treated in this study, several examples are examined, and the results are presented in graphical form. The homogeneous counterpart for a linearly hardening shaft was the subject of the investigation carried out by Gamer and Lance (1983). Nevertheless, the analytical solution for free ends is more complicated.

Formulation

Cylindrical polar coordinates (r, θ, z) are considered. The notation of Timoshenko and Goodier (1970) is used. Hence, in the formulation, σ_j and ϵ_j denote a normal stress and a normal strain component, respectively, u is the radial component of the displacement vector, and ρ and ω are the mass density and constant angular speed of rotation, respectively. Furthermore, a state of generalized plane strain, i.e. $\epsilon_z = \textit{constant,}$ and infinitesimal deformations are supposed. In addition the shaft is assumed to be sufficiently long compared with its outer diameter and so the end effects are negligible. In the plastic regions total strains are expressed as the superposition of elastic and plastic parts in the form

$$\epsilon_j = \epsilon_j^e + \epsilon_j^p, \tag{2}$$

where the superscripts e and p denote elastic and plastic, respectively.

Elastic Region

Strain-displacement relations for small strains, and the equations of generalized Hooke's law together with the equation of equilibrium in the radial direction:

$$\frac{d}{dr}(r\sigma_r) - \sigma_\theta + \rho\omega^2 r^2 = 0, \tag{3}$$

are valid throughout (Timoshenko and Goodier, 1970). The stress-displacement relations take the forms for the radial and circumferential components, respectively, as

$$\sigma_r = \frac{E_0}{(1+\nu)(1-2\nu)} \left(\frac{r}{b}\right)^n \left[\nu\epsilon_z + \frac{\nu}{r}u + (1-\nu)u'\right], \tag{4}$$

$$\sigma_\theta = \frac{E_0}{(1+\nu)(1-2\nu)} \left(\frac{r}{b}\right)^n \left[\nu\epsilon_z + \frac{(1-\nu)}{r}u + \nu u'\right], \tag{5}$$

and from Hooke's law

$$\sigma_z = E_0 \left(\frac{r}{b}\right)^n \epsilon_z + \nu\left(\sigma_r + \sigma_\theta\right). \tag{6}$$

In the expressions above, a prime denotes differentiation with respect to the radial coordinate. Substitution of Eqs. (4) and (5) into the equation of equilibrium, Eq. (3), leads to the elastic equation

$$r^2\frac{d^2u}{dr^2} + (1+n)r\frac{du}{dr} - \frac{1-\nu\,(1+n)}{1-\nu}u = -\frac{(1+\nu)\,(1-2\nu)\,b^n}{(1-\nu)E_0}r^{3-n}\rho\omega^2 - \frac{nr\nu\epsilon_z}{1-\nu}, \tag{7}$$

with the general solution

$$u(r) = C_1 r^{-(n+K)/2} + C_2 r^{-(n-K)/2} - \frac{(1+\nu)\,(1-2\nu)\,b^n r^{3-n}\rho\omega^2}{[8-3n-4(2-n)\nu]\,E_0} - r\nu\epsilon_z. \tag{8}$$

in which C_1 and C_2 represent arbitrary integration constants and the symbol K has been defined as

$$K = \sqrt{4+n^2-\frac{4n\nu}{1-\nu}}. \tag{9}$$

The stresses become

$$\begin{aligned}\sigma_r &= -\frac{E_0}{2\,(1+\nu)\,(1-2\nu)\,b^n}r^{(-2-K+n)/2}\left\{C_1\left[(K+n)\,(1-\nu)-2\nu\right]\right.\\ &\left.+C_2 r^K\left[(n-K)\,(1-\nu)-2\nu\right]\right\} - \frac{[3-n(1-\nu)-2\nu]\,r^2\rho\omega^2}{8-3n-4\nu(2-n)},\end{aligned} \tag{10}$$

$$\begin{aligned}\sigma_\theta &= \frac{E_0}{2\,(1+\nu)\,(1-2\nu)\,b^n}r^{(-2-K+n)/2}\left\{C_1\left[2-(2+K+n)\,\nu\right]\right.\\ &\left.+C_2 r^K\left[2-(2-K+n)\,\nu\right]\right\} - \frac{[1+(2-n)\nu]\,r^2\rho\omega^2}{8-3n-4\nu(2-n)},\end{aligned} \tag{11}$$

$$\begin{aligned}\sigma_z &= -\frac{(4-n)\nu r^2\rho\omega^2}{8\,(1-\nu)-n\,(3-4\nu)} + \frac{\nu E_0}{2\,(1+\nu)\,(1-2\nu)\,b^n}r^{(-2-K+n)/2}\\ &\times\left[C_1(2-K-n)+C_2 r^K(2+K-n)\right] + \frac{r^n E_0\epsilon_z}{b^n}.\end{aligned} \tag{12}$$

It is noted that, although this solution is used throughout this work, it is not finite only when $8-3n-4(2-n)\nu=0$. From $8-3n-4(2-n)\nu=0$, the critical value of the material parameter is determined as

$$n = n_C = \frac{8(1-\nu)}{3-4\nu}. \tag{13}$$

As an example, for $\nu = 3/10$, the critical value is $n_C = 28/9$. Although, as indicated earlier, parameter values as large as $n = 28/9$ are not considered in this work, the exact solution at $n = n_C$ may be derived. For $n = 8(1-\nu)/(3-4\nu)$, the elastic equation, Eq. (7), takes the form

$$\begin{aligned}r^2\frac{d^2u}{dr^2} + \left(3+\frac{2}{3-4\nu}\right)r\frac{du}{dr} - \frac{3(1-4\nu)}{3-4\nu}u &= -\frac{b^{2-2/(3-4\nu)}r^{1-2/(3-4\nu)}(1+\nu)(1-2\nu)\rho\omega^2}{(1-\nu)E_0}\\ &-\frac{8r\nu\epsilon_z}{3-4\nu},\end{aligned} \tag{14}$$

and assumes the exact solution

$$u(r)=\frac{\widehat{C}_1}{r^3}+\widehat{C}_2 r^{1-2/(3-4\nu)}+\frac{b^{2+2/(3-4\nu)}r^{1-2/(3-4\nu)}\widehat{D}\left[3-4\nu-2\left(5-8\nu\right)\ln r\right]\rho\omega^2}{4(1-\nu)(5-8\nu)^2E_0}-r\nu\epsilon_z, \tag{15}$$

where

$$\widehat{D}=(1+\nu)(1-2\nu)(3-4\nu). \tag{16}$$

Since the ends of the shaft are free, it contracts as it rotates. The net force F_z in the axial direction should vanish, and this condition allows one to determine the constant axial strain ϵ_z. Assuming that the elastic region is confined in $\alpha\leq r\leq\beta$, with the help of Eq. (12) the axial force is determined as

$$\begin{aligned}F_{ze}(\alpha,\beta) &= \int_\alpha^\beta r\sigma_z dr=\frac{B_1}{4}\left(\beta^4-\alpha^4\right)+\frac{2B_2\left[\beta^{(2-K+n)/2}-\alpha^{(2-K+n)/2}\right]}{2-K+n}\\ &+\frac{2B_3\left[\beta^{(2+K+n)/2}-\alpha^{(2+K+n)/2}\right]}{2+K+n}+\frac{\left(\beta^{2+n}-\alpha^{2+n}\right)E_0\epsilon_z}{(2+n)\,b^n},\end{aligned} \tag{17}$$

where

$$B_1=-\frac{(4-n)\,\nu\rho\omega^2}{8\,(1-\nu)-n\,(3-4\nu)}, \tag{18}$$

$$B_2=\frac{C_1\,(2-K-n)\,\nu E_0}{2\,(1+\nu)\,(1-2\nu)\,b^n}, \tag{19}$$

$$B_3=\frac{C_2\,(2+K-n)\,\nu E_0}{2\,(1+\nu)\,(1-2\nu)\,b^n}. \tag{20}$$

Plastic Region I

In this region the stress state satisfies $\sigma_\theta>\sigma_z>\sigma_r$. Accordingly, Tresca's yield criterion reads

$$\sigma_\theta-\sigma_r=\sigma_0, \tag{21}$$

with σ_0 being the uniaxial elastic limit of the material. The flow rule associated with this yielding is $\epsilon_\theta^p=-\epsilon_r^p$, and $\epsilon_z^p=0$. Making use of $\epsilon_z^p=0$ and expressing the stresses in terms of the radial stress σ_r one arrives at $\sigma_\theta=\sigma_0+\sigma_r$, and

$$\sigma_z=E(r)\epsilon_z+\nu\left(\sigma_0+2\sigma_r\right). \tag{22}$$

Using the equation of equilibrium, Eq. (3), and the condition $\sigma_r(a)=0$ we obtain the expressions for the stress components as

$$\sigma_r=-\frac{\left(r^2-a^2\right)}{2}\rho\omega^2+\sigma_0\ln\left(r/a\right), \tag{23}$$

$$\sigma_\theta=-\frac{\left(r^2-a^2\right)}{2}\rho\omega^2+\sigma_0\left[1+\ln\left(r/a\right)\right], \tag{24}$$

$$\begin{aligned}\sigma_z &= -(r^2-a^2)\nu\rho\omega^2+\left(\frac{r}{b}\right)^n E_0\epsilon_z\\ &+\nu\left[1+2\ln\left(r/a\right)\right]\sigma_0.\end{aligned} \tag{25}$$

The stress expressions together with strain-displacement relations and the associated flow rule show the way for the nonhomogeneous differential equation

$$\frac{du}{dr}+\frac{u}{r}=-2\nu\epsilon_z+\frac{1}{E_0}\left(\frac{r}{b}\right)^{-n}(1+\nu)\,(1-2\nu)\left\{\left(a^2-r^2\right)\rho\omega^2+\left[1+2\ln\left(r/a\right)\right]\sigma_0\right\}. \tag{26}$$

The solution is

$$\begin{aligned}u &= \frac{C_3}{r}-r\nu\epsilon_z-\frac{(1+\nu)(1-2\nu)b^n}{(2-n)E_0}r^{1-n}\left\{\frac{[(2-n)r^2-a^2(4-n)]\rho\omega^2}{4-n}\right.\\ &\left.+\frac{[n-2(2-n)\ln\left(r/a\right)]\sigma_0}{2-n}\right\}.\end{aligned} \tag{27}$$

Finally, the plastic strains and the force integral are obtained, respectively, as

$$\begin{aligned}\epsilon_\theta^p &= -\epsilon_r^p = \frac{C_3}{r^2} + \frac{\left[(2-n)^2 r^2 + a^2 n(4-n)\right](1+\nu)(1-2\nu) b^n \rho\omega^2}{2(4-n)(2-n) r^n E_0} \\ &\quad -\frac{(1+\nu) b^n \sigma_0}{(2-n)^2 r^n E_0}\left\{4(1-\nu) - n\left[3 - n(1-\nu) - 2\nu\right] - n(2-n)(1-2\nu)\ln(r/a)\right\}, \end{aligned} \tag{28}$$

$$\begin{aligned} F_{zI}(\alpha,\beta) &= -\frac{1}{4}\left(\beta^2-\alpha^2\right)\left(\alpha^2+\beta^2-2a^2\right)\nu\rho\omega^2 + \frac{\left(\beta^{2+n}-\alpha^{2+n}\right)E_0\epsilon_z}{(2+n)b^n} \\ &\quad -\nu\left[\alpha^2\ln\left(\frac{\alpha}{a}\right) - \beta^2\ln\left(\frac{\beta}{a}\right)\right]\sigma_0. \end{aligned} \tag{29}$$

Plastic Region II

This is a corner regime, where the stresses satisfy $\sigma_\theta > \sigma_z = \sigma_r$. Tresca's yield condition becomes

$$\sigma_\theta - \sigma_r = \sigma_\theta - \sigma_z = \sigma_0. \tag{30}$$

The associated flow rule is $\epsilon_\theta^p = -\left(\epsilon_r^p + \epsilon_z^p\right)$. Hence, by the use of the equation of equilibrium

$$\sigma_r = \sigma_z = -\frac{r^2\rho\omega^2}{2} + (C_4 + \ln r)\,\sigma_0, \tag{31}$$

$$\sigma_\theta = -\frac{r^2\rho\omega^2}{2} + (1 + C_4 + \ln r)\,\sigma_0. \tag{32}$$

On the other hand, the plastic strain in the axial direction is determined as

$$\epsilon_z^p = \epsilon_z + \frac{b^n\left\{(1-2\nu) r^2\rho\omega^2 + 2\left[\nu - (1-2\nu)(C_4+\ln r)\right]\sigma_0\right\}}{2r^n E_0}. \tag{33}$$

Making use of the strain-displacement relations, the stress expressions, i.e. Eqs. (31) and (32), and the associated flow rule, i.e. $\epsilon_r^p + \epsilon_\theta^p = -\epsilon_z^p$, we arrive at

$$\frac{du}{dr} + \frac{u}{r} = -\epsilon_z - \frac{b^n(1-2\nu)\left[3r^2\rho\omega^2 - 2(1+3C_4+3\ln r)\sigma_0\right]}{2r^n E_0}. \tag{34}$$

The general solution of this equation is

$$\begin{aligned} u &= \frac{C_5}{r} - \frac{r\epsilon_z}{2} - \frac{(1-2\nu) b^n r^{1-n}}{2(4-n)(2-n)^2 E_0}\left\{3(2-n)^2 r^2\rho\omega^2\right. \\ &\quad \left. +2(4-n)\left[1 - 3C_4(2-n) + n - 3(2-n)\ln r\right]\sigma_0\right\}. \end{aligned} \tag{35}$$

The axial plastic strain has already been given by Eq. (33). Subtracting elastic strain from the total the plastic strain in the circumferential direction is obtained. The result is

$$\begin{aligned}\epsilon_\theta^p &= \frac{C_5}{r^2} + \frac{(1-2\nu)(1-n) b^n r^{2-n}\rho\omega^2}{2(4-n)E_0} - \frac{\epsilon_z}{2} \\ &\quad -\frac{b^n\sigma_0}{(2-n) r^n E_0}\left[\frac{5+n^2-2\nu-n(3+2\nu)}{2-n} - (1-2\nu)(1+n)(C_4+\ln r)\right]. \end{aligned} \tag{36}$$

From the associated flow rule

$$\begin{aligned}\epsilon_r^p &= \frac{b^n(1-2\nu)}{2E_0 r^n}\left[\frac{2C_4(1-2n)\sigma_0}{2-n} - \frac{(5-2n)\rho\omega^2 r^2}{4-n}\right] - \frac{C_5}{r^2} - \frac{\epsilon_0}{2} \\ &\quad +\frac{b^n\sigma_0}{(2-n)^2 E_0 r^n}\{5 - n\left[3 - n(1-\nu) - 2\nu\right] - 6\nu + (2-n)(1-2n)(1-2\nu)\ln r\}. \end{aligned} \tag{37}$$

Finally, the force integral for this region is evaluated as

$$F_{zII}(\alpha,\beta)=\frac{1}{8}\left\{-\left(\beta^4-\alpha^4\right)\rho\omega^2-2\left[\left(1-2C_4\right)\left(\beta^2-\alpha^2\right)+2\alpha^2\ln\alpha-2\beta^2\ln\beta\right]\sigma_0\right\}. \tag{38}$$

Plastic Region III

In this plastic region the stress state satisfies the inequality $\sigma_\theta>\sigma_r>\sigma_z$. Tresca's yield condition takes the form

$$\sigma_\theta-\sigma_z=\sigma_0. \tag{39}$$

The flow rule associated with this yield condition is $\epsilon_\theta^p=-\epsilon_z^p$, and $\epsilon_r^p=0$. Making use of the flow rule, a straightforward manipulation of the equations of Hooke's law yields the following stress-displacement relations

$$\sigma_r=\frac{E_0}{(1+\nu)(1-2\nu)b^n}\left[r^{-1+n}\nu\left(r\epsilon_z+u\right)+r^n(1-\nu)u'\right], \tag{40}$$

$$\sigma_\theta=\frac{\sigma_0}{2}+\frac{E_0}{2(1+\nu)(1-2\nu)b^n}r^{-1+n}[r\epsilon_z+u+2r\nu u']. \tag{41}$$

Inserting Eqs. (40) and (41) into the equation of equilibrium gives the governing equation for this region

$$\begin{aligned} r^2\frac{d^2u}{dr^2}+(1+n)r\frac{du}{dr}-\frac{1-2n\nu}{2(1-\nu)}u &= \frac{r\left[1-2(1+n)\nu\right]\epsilon_z}{2(1-\nu)} \\ &\quad -\frac{b^nr^{1-n}(1+\nu)(1-2\nu)\left(2r^2\rho\omega^2-\sigma_0\right)}{2(1-\nu)E_0}. \end{aligned} \tag{42}$$

The general solution is simplified to

$$\begin{aligned} u &= C_6r^{-(n+L)/2}+C_7r^{-(n-L)/2}+\frac{2r\left[1-2(1+n)\nu\right]\epsilon_z}{(2-L+n)(2+L+n)(1-\nu)} \\ &\quad -\frac{2(1+\nu)(1-2\nu)b^nr^{1-n}}{(1-\nu)E_0}\left[\frac{2r^2\rho\omega^2}{(6+L-n)(6-L-n)}-\frac{\sigma_0}{(2+L-n)(2-L-n)}\right], \end{aligned} \tag{43}$$

where

$$L=\sqrt{n(4+n)+\frac{2(1-2n)}{1-\nu}}. \tag{44}$$

The stresses are shown by

$$\begin{aligned} \sigma_r &= -\frac{2\left[3-n(1-\nu)-2\nu\right]r^2\rho\omega^2}{17-18\nu-2n(3-4\nu)}+\frac{r^nE_0\epsilon_z}{\left[1+2(n-\nu)\right]b^n}+\frac{\left[1-n(1-\nu)\right]\sigma_0}{(1-2n)(1-2\nu)} \\ &\quad -\frac{E_0}{2(1+\nu)(1-2\nu)b^n}r^{(-2-L+n)/2}\left\{C_6\left[(L+n)(1-\nu)-2\nu\right]\right. \\ &\quad \left.+C_7r^L\left[(n-L)(1-\nu)-2\nu\right]\right\}, \end{aligned} \tag{45}$$

$$\begin{aligned} \sigma_\theta &= -\frac{\left[1+2(3-n)\nu\right]r^2\rho\omega^2}{17-18\nu-2n(3-4\nu)}+\frac{(1+n)r^nE_0\epsilon_z}{\left[1+2(n-\nu)\right]b^n}+\frac{\left[1-n(1-\nu)\right]\sigma_0}{(1-2n)(1-2\nu)} \\ &\quad +\frac{E_0}{2(1+\nu)(1-2\nu)b^n}r^{(-2-L+n)/2}\left\{C_6\left[1-(L+n)\nu\right]+C_7r^L\left[1+(L-n)\nu\right]\right\}, \end{aligned} \tag{46}$$

$$\sigma_z = -\frac{[1+2(3-n)\nu]r^2\rho\omega^2}{17-18\nu-2n(3-4\nu)} + \frac{(1+n)r^nE_0\epsilon_z}{[1+2(n-\nu)]b^n} + \frac{[n+\nu(2-3n)]\sigma_0}{(1-2n)(1-2\nu)} + \frac{E_0}{2(1+\nu)(1-2\nu)b^n} r^{(-2-L+n)/2}\left\{C_6[1-(L+n)\nu] + C_7 r^L[1+(L-n)\nu]\right\}. \quad (47)$$

The plastic strain and the force integral expressions are then determined. The results are

$$\epsilon_\theta^p = -\epsilon_z^p = \frac{1}{2}r^{(-2-L-n)/2}\left(C_6 + C_7 r^L\right) - \frac{(1+\nu)(1-2\nu)b^n r^{2-n}\rho\omega^2}{[17-18\nu-2n(3-4\nu)]E_0} - \frac{(1+\nu)n\epsilon_z}{1+2(n-\nu)} + \frac{(1+\nu)nb^n\sigma_0}{(1-2n)r^nE_0}, \quad (48)$$

$$F_{zIII}(\alpha,\beta) = \frac{D_1}{4}\left(\beta^4-\alpha^4\right) + \frac{2D_2\left[\beta^{(2+L+n)/2}-\alpha^{(2+L+n)/2}\right]}{2+L+n} + \frac{2D_3\left[\beta^{(2-L+n)/2}-\alpha^{(2-L+n)/2}\right]}{2-L+n} + \frac{D_4}{2}\left(\beta^2-\alpha^2\right) + \frac{(1+n)\left(\beta^{2+n}-\alpha^{2+n}\right)E_0\epsilon_z}{(2+n)[1+2(n-\nu)]b^n}, \quad (49)$$

in which

$$D_1 = -\frac{[1+2(3-n)\nu]\rho\omega^2}{17-18\nu-2n(3-4\nu)}, \quad (50)$$

$$D_2 = \frac{C_7[1+\nu(L-n)]E_0}{2(1+\nu)(1-2\nu)b^n}, \quad (51)$$

$$D_3 = \frac{C_6[1-\nu(L+n)]E_0}{2(1+\nu)(1-2\nu)b^n}, \quad (52)$$

$$D_4 = \frac{[n+\nu(2-3n)]\sigma_0}{(1-2n)(1-2\nu)}. \quad (53)$$

Elastic and Elastic-plastic Deformations

Elastic deformation

Using traction free boundary conditions, $\sigma_r(a) = \sigma_r(b) = 0$, the integration constants are evaluated as

$$C_1 = \frac{2\left[a^Kb^{(6+K+n)/2} - a^{(6+K-n)/2}b^{K+n}\right][3-n(1-\nu)-2\nu](1+\nu)(1-2\nu)\rho\omega^2}{(b^K-a^K)[(K+n)(1-\nu)-2\nu][8(1-\nu)-n(3-4\nu)]E_0}, \quad (54)$$

$$C_2 = -\frac{2\left[a^{(6+K-n)/2}b^n - b^{(6+K+n)/2}\right][3-n(1-\nu)-2\nu](1+\nu)(1-2\nu)\rho\omega^2}{(b^K-a^K)[(K-n)(1-\nu)+2\nu][8(1-\nu)-n(3-4\nu)]E_0}. \quad (55)$$

The expression for the axial force, Eq. (17), is used to find ϵ_z. Setting $F_{ze}(a,b) = 0$, the result is

$$\epsilon_z = -\frac{b^n(b^4-a^4)(2+n)\nu\rho\omega^2}{4(b^{2+n}-a^{2+n})E_0}. \quad (56)$$

Note that for $n = 0$ this expression reduces to the familiar one (Eraslan, 2004):

$$\epsilon_z = -\frac{(a^2+b^2)\nu\rho\omega^2}{2E_0}. \tag{57}$$

Yielding commences at the inner surface as soon as $\sigma_\theta(a) = \sigma_0$. After some algebraic manipulations, the elastic limit angular speed is determined as

$$\Omega_e = \sqrt{\frac{ab^{(4+n)/2}(b^K - a^K)[8 - 3n - 4(2-n)\nu]S_1S_2}{(1-2\nu)\left\{4a^{(n+K)/2}b^{(6+K)/2}S_3 + a^3b^{n/2}[b^K(n-K-6)S_1 - a^K(6-K-n)S_2]\right\}}}, \tag{58}$$

in which Ω is the nondimensional angular speed defined by $\Omega = \omega b(\rho/\sigma_0)^{1/2}$ and

$$S_1 = K - n(1-\nu) + (2-K)\nu, \tag{59}$$

$$S_2 = K + n - (2 + K + n)\nu, \tag{60}$$

$$S_3 = K[3 - n(1-\nu) - 2\nu]. \tag{61}$$

A validation of Eq. (58) is performed by the substitution of $n = 0$. The result is

$$\Omega_e = \sqrt{\frac{4(1-\nu)}{\overline{a}^2(1-2\nu) + 3 - 2\nu}} \tag{62}$$

where $\overline{a} = a/b$ denotes nondimensional bore radius (Mack, 1991a; Eraslan, 2004).

First stage of elastic-plastic deformation

In the first stage, the shaft consists of an inner plastic region (region I) in $a \le r \le r_1$, and an outer elastic region in $r_1 \le r \le b$, with r_1 being the border radius separating plastic and elastic regions. The solution of this problem necessitates the evaluation of 5 unknowns: integration constants C_3 (plastic I), C_1, C_2 (elastic), border radius r_1, and axial strain ϵ_z. The following 4 conditions are valid: 1. $\sigma_r^{pI}(r_1) = \sigma_r^e(r_1)$; 2. $u_r^{pI}(r_1) = u_r^e(r_1)$; 3. $\sigma_\theta^e(r_1) - \sigma_r^e(r_1) = \sigma_0$; 4. $\sigma_r^e(b) = 0$, where the superscripts pI and e stand for plastic I and elastic regions, respectively. Another condition concerning the evaluation of ϵ_z is obtained by the help of force integrals. Using Eqs. (17) and (29) we set $F_{zI}(a, r_1) + F_{ze}(r_1, b) = 0$ to get

$$\begin{aligned}\epsilon_z = R_1 \;=\; & \frac{(2+n)\,b^n}{(b^{2+n} - a^{2+n})\,E_0}\left\{-\frac{2B_2\left[b^{(2-K+n)/2} - r_1^{(2-K+n)/2}\right]}{2-K+n}\right. \\ & -\frac{2B_3\left[b^{(2+K+n)/2} - r_1^{(2+K+n)/2}\right]}{2+K+n} + \frac{1}{4}\left[\left(r_1^2 - a^2\right)^2\nu\rho\omega^2 - B_1\left(b^4 - r_1^4\right)\right] \\ & \left. - \ln\left(\frac{r_1}{a}\right)\nu r_1^2\sigma_0\right\},\end{aligned} \tag{63}$$

in which the symbols K, B_1, B_2, and B_3 have already been defined in the Elastic Solution Section by Eqs. (9) and (18)-(20). The fifth condition is therefore: 5. $\epsilon_z - R_1 = 0$. The expressions obtained upon application of these conditions result in a 5×5 system, which is nonlinear in r_1 and linear in the other unknowns. The simultaneous solution of this system is achieved by Newton iterations.

Second stage of elastic-plastic deformation

The shaft is composed of 3 adjacent plastic zones: plastic I in $a \le r \le r_1$, plastic II in $r_1 \le r \le r_2$, plastic III in $r_2 \le r \le r_3$, and an outer elastic region in $r_3 \le r \le b$. The solution of this deformation stage requires the calculation of 11 unknowns. These are C_3 (plastic I), C_4, C_5 (plastic II), C_6, C_7 (plastic III), C_1, C_2 (elastic), r_1, r_2, r_3, and ϵ_z. Boundary condition 4 in the first stage is

still valid, and we add the following continuity conditions: 1. $\sigma_r^{pI}(r_1) = \sigma_r^{pII}(r_1)$; 2. $u_r^{pI}(r_1) = u_r^{pII}(r_1)$; 3. $\sigma_\theta^{pI}(r_1) - \sigma_z^{pI}(r_1) = \sigma_0$; 5. $\sigma_r^{pII}(r_2) = \sigma_r^{pIII}(r_2)$; 6. $u_r^{pII}(r_2) = u_r^{pIII}(r_2)$; 7. $\sigma_\theta^{pIII}(r_2) - \sigma_r^{pIII}(r_2) = \sigma_0$; 8. $\sigma_r^{pIII}(r_3) = \sigma_r^e(r_3)$; 9. $u_r^{pIII}(r_3) = u_r^e(r_3)$; 10. $\sigma_\theta^e(r_3) - \sigma_z^e(r_3) = \sigma_0$; and 11. $\epsilon_z - R_2 = 0$. Here, the superscripts pII and $pIII$ stand for regions plastic II and plastic III, respectively. Furthermore, R_2 is the outcome of stating

$$F_{zI}(a, r_1) + F_{zII}(r_1, r_2) + F_{zIII}(r_2, r_3) + F_{ze}(r_3, b) = 0, \tag{64}$$

given by

$$\begin{aligned} R_2 \;=\; & \frac{(2+n)\, b^n}{\left[b^{2+n} - r_3^{2+n} + r_1^{2+n} - a^{2+n} + \frac{(1+n)\left(r_3^{2+n} - r_2^{2+n}\right)}{1+2(n-\nu)}\right] E_0} \left\{ \frac{1}{8}\left[r_2^4 - r_1^4 + 2\nu\left(a^2 - r_1^2\right)^2\right]\rho\omega^2 \right. \\ & - \frac{B_1}{4}\left(b^4 - r_3^4\right) - \frac{2B_2\left[b^{(2-K+n)/2} - r_3^{(2-K+n)/2}\right]}{2-K+n} - \frac{2B_3\left[b^{(2+K+n)/2} - r_3^{(2+K+n)/2}\right]}{2+K+n} \\ & - \frac{D_1}{4}\left(r_3^4 - r_2^4\right) - \frac{2D_2\left[r_3^{(2+L+n)/2} - r_2^{(2+L+n)/2}\right]}{2+L+n} - \frac{2D_3\left[r_3^{(2-L+n)/2} - r_2^{(2-L+n)/2}\right]}{2-L+n} \\ & - \frac{D_4}{2}\left(r_3^2 - r_2^2\right) + \frac{C_4}{2}\left(r_1^2 - r_2^2\right)\sigma_0 - \frac{1}{4}\left[\left(1 - 2\ln r_1 + 4\nu \ln\left(\frac{r_1}{a}\right)\right) r_1^2 \right. \\ & \left. \left. - \left(1 - 2\ln r_2\right) r_2^2\right]\sigma_0 \right\}, \end{aligned} \tag{65}$$

where the symbols L, D_1, D_2, D_3, and D_4 have been defined by Eqs. (44) and (50)-(53).

Third stage of elastic-plastic deformation

In this last stage of elastic-plastic deformation the shaft consists of 2 adjacent plastic regions: plastic II in $a \le r \le r_2$, plastic III in $r_2 \le r \le r_3$, and an elastic region in $r_3 \le r \le b$. The unknowns to be determined for the solution are C_4, C_5 (plastic II), C_6, C_7 (plastic III), C_1, C_2 (elastic), r_2, r_3, and ϵ_z. Condition 4 in the first stage and conditions 5-10 in the second stage are still applicable. In addition, we have $\sigma_r^{pII}(a) = 0$, and $\epsilon_z - R_3 = 0$, where

$$\begin{aligned} R_3 \;=\; & \frac{b^n\,(2+n)\left[1 + 2\,(n-\nu)\right]}{\left\{b^{2+n}\left[1 + 2\,(n-\nu)\right] - (1+n)\, r_2^{2+n} - (n-2\nu)\, r_3^{2+n}\right\} E_0} \left\{ \frac{\left(r_2^4 - a^4\right)}{8}\rho\omega^2 \right. \\ & + \left[r_2^2\left(1 - 2C_4 - 2\ln r_2\right) - a^2\left(1 - 2C_4 - 2\ln a\right)\right]\frac{\sigma_0}{4} - \frac{D_1}{4}\left(r_3^4 - r_2^4\right) \\ & - \frac{2D_2\left[r_3^{(2+L+n)/2} - r_2^{(2+L+n)/2}\right]}{2+L+n} - \frac{2D_3\left[r_3^{(2-L+n)/2} - r_2^{(2-L+n)/2}\right]}{2-L+n} - \frac{D_4}{2}\left(r_3^2 - r_2^2\right) \\ & \left. - \frac{B_1}{4}\left(b^4 - r_3^4\right) - \frac{2B_2\left[b^{(2-K+n)/2} - r_3^{(2-K+n)/2}\right]}{2-K+n} - \frac{2B_3\left[b^{(2+K+n)/2} - r_3^{(2+K+n)/2}\right]}{2+K+n} \right\}, \end{aligned} \tag{66}$$

which is obtained from $F_{zII}(a, r_2) + F_{zIII}(r_2, r_3) + F_{ze}(r_3, b) = 0$.

Results and Discussion

The Poisson's ratio is taken as $\nu = 0.3$ in the subsequent calculations. What's more, formal nondimen-

sional and normalized variables given by radial coordinate $\overline{r} = r/b$, stress $\overline{\sigma}_j = \sigma_j/\sigma_0$, radial displacement $\overline{u} = uE_0/(\sigma_0 b)$, and strain $\overline{\epsilon}_j = \epsilon_j E_0/\sigma_0$ are used for the presentation of results. For consistency the integration constants are reported in dimensionless forms as well. They are $\overline{C}_1 = C_1/b^{1+(n+K)/2}$, $\overline{C}_2 = C_2/b^{1+(n-K)/2}$, $\overline{C}_3 = C_3/b^2$, $\overline{C}_4 = C_4$, $\overline{C}_5 = C_5/b^2$, $\overline{C}_6 = C_6/b^{1+(n+L)/2}$, and $\overline{C}_7 = C_7/b^{1+(n-L)/2}$.

First, the verification of the complete solution will be performed in comparison to Mack's (1991a). This can be accomplished by taking $n = 0$. However unfortunately, because of the appearance of terms $2-K+n$ in the denominators of Eqs. (63) and (65)-(66) this cannot be done exactly. It is obvious that, for $n = 0$, $K = 2$, and hence $2 - K + n = 0$! However, a numerical limit may be taken considering a sufficiently small value of the material parameter n.

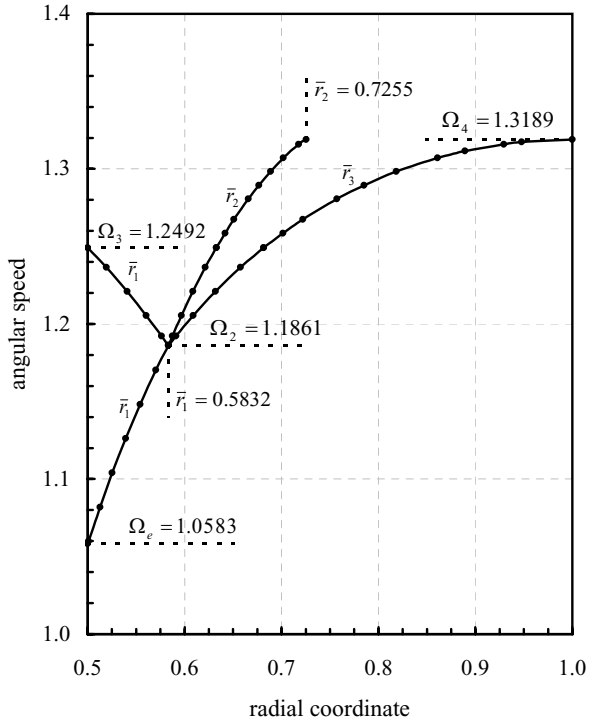

Figure 1. Evolution of plastic regions with increasing Ω for $n = 10^{-5}$. Solid lines show present calculation ($n = 10^{-5}$) and dots belong to the analytical solution of Mack (1991a) for a homogeneous shaft ($n = 0$).

Considering a hollow shaft of inner radius $a/b = 0.5$ and setting n as low as 10^{-5} all 3 stages of elastoplastic deformations are solved to obtain the evolution of plastic regions as well as critical values of the parameters during transitions from one stage to another. The results are shown in Figure 1. In this figure, the solid lines represent the present calculation and the dots are from Mack (1991b). It is noted that, in Figure 3 of Mack's article, the ordinate shows Ω^2 values, rather than Ω. Both solutions do agree well. In fact, most of the critical numbers indicated in this figure agree with those of Mack in all the digits displayed. The formation of each of the plastic regions, and their expansion over each other and toward the edge can clearly be evaluated by a careful examination of Figure 1.

Similar comprehensive calculations are also performed for FGM shafts of $a/b = 0.5$ using the material parameter values $n = 0.4$ and $n = -0.4$. The results of these calculations are shown in Figure 2 together with the results of a homogeneous one (dashed lines). In addition, the critical values of the parameters obtained during these calculations are summarized in Table 1.

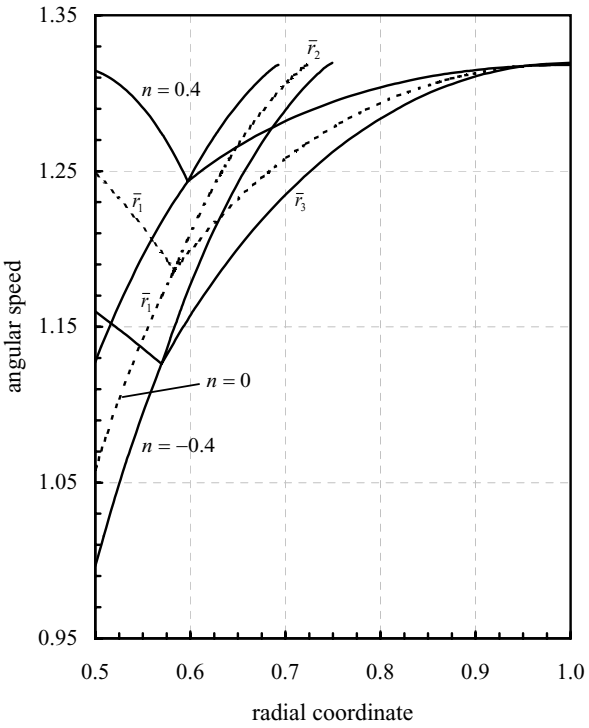

Figure 2. Evolution of plastic regions in FGM shafts with increasing Ω for $n = -0.4$, and $n = 0.4$ in comparison to that in a homogeneous one (dashed lines).

It is interesting to note that, although the intermediate limits Ω_e, Ω_2, and Ω_3 differ notably, as shown in Table 1, the fully plastic limits, Ω_4 values, are just about the same. Hence, it can be stated that

the fully plastic limit of a rotating FGM hollow shaft with free ends is almost independent of the variation in the modulus of elasticity in the shaft material.

Table 1. Limit angular speeds for FGM and homogeneous shafts.

Limits	$n=-0.4$	$n=0$	$n=0.4$
Ω_e	0.9965	1.0583	1.1273
Ω_2	1.1262	1.1861	1.2434
$\overline{r}_1$ (at Ω_2)	0.5699	0.5832	0.5973
Ω_3	1.1599	1.2492	1.3145
Ω_4	1.3194	1.3189	1.3182
$\overline{r}_2$ (at Ω_4)	0.7493	0.7255	0.6927

Using Eq. (58), the elastic limit angular speeds for FGM shafts of different inner radius are calculated as a function of the material parameter n, and plotted in Figure 3. For all $\overline{a}$, the elastic limits increase with increasing values of n, and for $n > 0$ the elastic limits are greater than the corresponding homogeneous ones. Hence, the strength of the shaft to elastically resist the centrifugal force increases if $E(r)$ increases in the radial direction from a to b. Calculations are performed in the elastic stress state to display the stresses. A hollow shaft of $a/b = 0.6$ is considered for this purpose. For $n = 0$, from Eqs. (58) and (54)-(56), in turn, we evaluate $\Omega_e = 1.0491$. The results of the calculations for $n = 0$ and 0.5 are summarized in Table 2.

Table 2. Calculated constants for $a/b = 0.6$ at $\Omega = 1.0491$.

Constants	$n=0$	$n=0.5$
$\overline{C}_1 \times 10^4$	4.41509	3.73334
$\overline{C}_2 \times 10^4$	6.67170	9.00729
$\overline{\epsilon}_z \times 10^4$	−4.49057	−4.98159

The corresponding distributions of stress and radial displacement in these 2 different shafts are presented in Figure 4 for comparison. Solid lines belong to the FGM shaft ($n = 0.5$) and dashed lines belong to the homogeneous one.

The two FGM shafts with $n = -0.4$ and $n = 0.4$, considered in Figure 2, are both partially plastic at the speed of rotation $\Omega = 1.3$. However, the one with $n = -0.4$ is in the third stage of elastic-plastic deformation, while the other for $n = 0.4$ is in the second stage, as seen in Figure 2. Elastoplastic calculations are performed for these FGM shafts at $\Omega = 1.3$. The results of these calculations are summarized in Table 3.

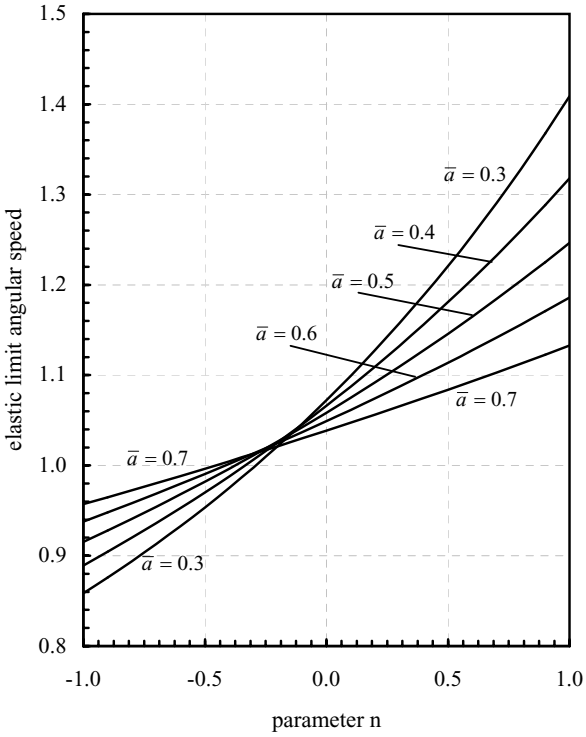

Figure 3. Variation of elastic limit angular speed Ω_e with material parameter n for FGM shafts of different inner radius.

Table 3. Calculated constants for $a/b = 0.5$ at $\Omega = 1.3$.

Constants	$n=-0.4$	$n=0.4$
$\overline{C}_3 \times 10^4$	–	9.05819
$\overline{r}_1$	–	0.535893
$\overline{C}_4$	0.904397	0.904397
$\overline{C}_5 \times 10^4$	7.92290	9.52451
$\overline{r}_2$	0.714673	0.659809
$\overline{C}_6 \times 10^4$	7.88932	6.43488
$\overline{C}_7 \times 10^2$	−0.166626	−1.16095
$\overline{r}_3$	0.851010	0.777955
$\overline{C}_1 \times 10^4$	6.91281	4.92267
$\overline{C}_2 \times 10^3$	0.804448	1.23825
$\overline{\epsilon}_z \times 10^4$	−7.08178	−7.31130

The matching stresses and displacements are depicted in Figure 5(a). The distribution of the plastic strains can be seen in Figure 5(b). The residual stresses $\overline{\sigma}_j^0$ upon complete unloading of the load $\Omega = 1.3$ (Figure 5(a)) are also calculated. Figure 5(c) shows the distributions of the maximum ($\overline{\sigma}_\theta^0$) and minimum ($\overline{\sigma}_r^0$) residual stress components at standstill. The residual plastic strains are not altered and are as given in Figure 5(b).

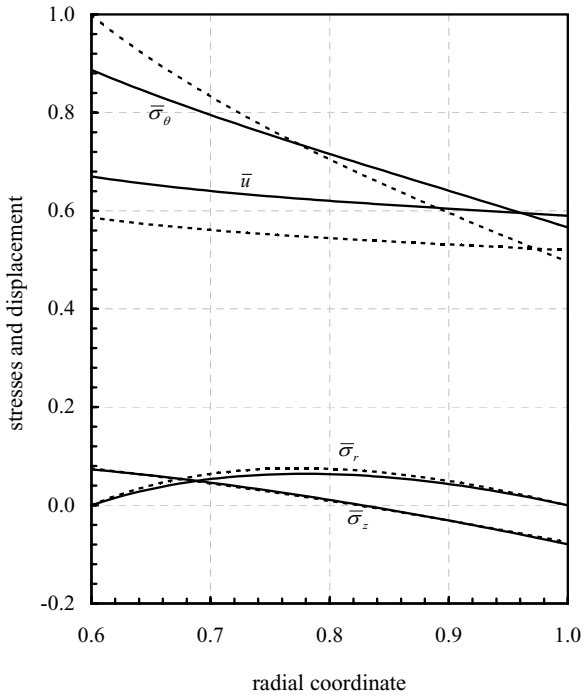

Figure 4. Stresses and displacement in the elastic stress state in an FGM shaft for $n = 0.5$ (solid lines) in comparison to those in a homogeneous one (dashed lines) at $\Omega = 1.0491$.

It has to be noted that the elastoplastic response of a rotating hollow shaft with axially constrained ends, i.e. $\epsilon_z = 0$, constitutes a different problem as the stress state in such a shaft satisfies $\sigma_\theta > \sigma_z > \sigma_r$ throughout (Gamer and Lance, 1983). Plastic deformation commences at the inner surface of the shaft according to Tresca's yield criterion $\sigma_\theta - \sigma_r = \sigma_0$ (plastic I) and this plastic region expands with increasing rotation speeds until the shaft becomes fully plastic. The succeeding corner regime (plastic II) and its accompanying side regime (plastic III) never appear. The stress and deformation expressions for the solution of this problem are readily obtained from those given in elastic and plastic I solutions by the substitution of $\epsilon_z = 0$. A shaft of $a/b = 0.5$ is taken into consideration. For $n = 0.6$ the elastic limit angular speed is calculated from Eq. (58) as $\Omega_e = 1.1648$. In addition, from Eqs. (54) and (55) we obtain $\overline{C}_1 = 3.38095 \times 10^{-4}$ and $\overline{C}_2 = 1.16630 \times 10^{-3}$. Conversely, at the speed $\Omega_e = 1.1648$ a homogeneous shaft is partially plastic. Hence, elastoplastic calculations are to be performed to find the stresses in a homogeneous shaft at $\Omega = 1.1648$. Since, Eq. (63) is not used in this calculation, the exact limit $n = 0$ is possible. Accordingly, for $n = 0$ we evaluate $\overline{C}_3 = 5.88266 \times 10^{-4}$, $\overline{r}_1 = 0.566210$, $\overline{C}_1 = 4.20190 \times 10^{-4}$, and $\overline{C}_2 = 8.18171 \times 10^{-4}$. The corresponding stresses are shown in Figure 6. The FGM shaft of $a/b = 0.5$ for $n = 0.6$ becomes partially plastic at speeds $\Omega > \Omega_e = 1.1648$. Assigning $\Omega = 1.25$ elastoplastic calculations are carried out. Two solution sets result: $\overline{C}_3 = 7.41858 \times 10^{-4}$, $\overline{r}_1 = 0.646698$, $\overline{C}_1 = 5.29899 \times 10^{-4}$, $\overline{C}_2 = 9.60620 \times 10^{-4}$ and $\overline{C}_3 = 9.35256 \times 10^{-4}$, $\overline{r}_1 = 0.57794$, $\overline{C}_1 = 4.00893 \times 10^{-4}$, $\overline{C}_2 = 1.35182 \times 10^{-3}$ for $n = 0$, and $n = 0.6$, respectively. Figure 7 shows the corresponding stresses and displacement. The expansion of the plastic region I in the FGM shafts as Ω increases is calculated as well. The results of these calculations are displayed in Figure 8. The advantage of using $n > 0$ is apparent. The fully plastic limit is exactly $\Omega = 1.35956$, and it turns out to be independent of the material parameter n.

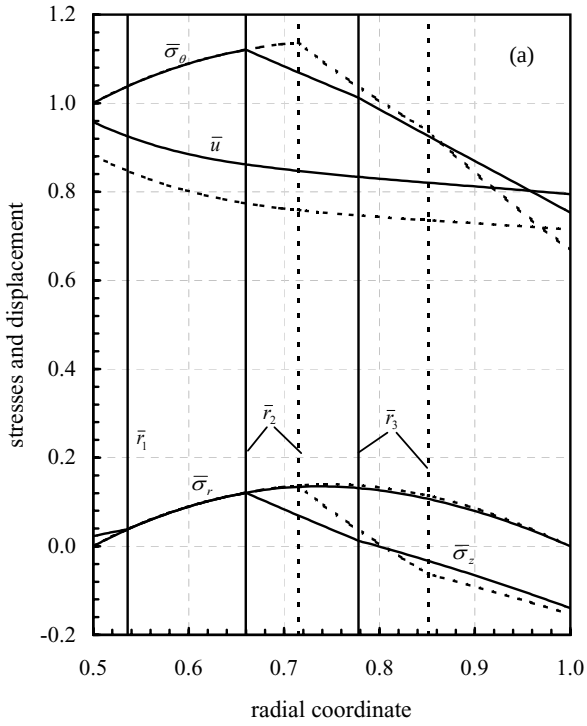

Figure 5. (a) Stresses and displacement, (b) plastic strains, (c) radial and circumferential residual stress components upon complete unloading in the partially plastic stress state in FGM shafts for $n = 0.4$ (solid lines), and $n = -0.4$ (dashed lines) at the rotation speed $\Omega = 1.3$.

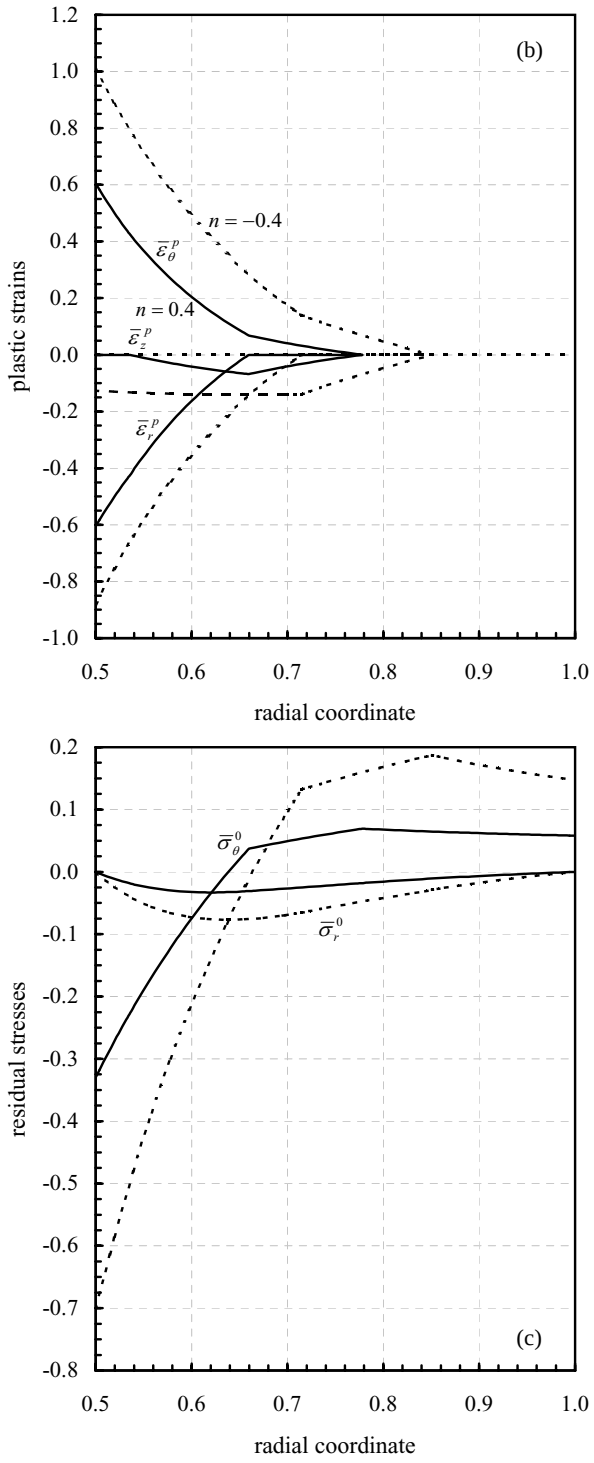

Figure 5. Contunied.

In the preceeding calculations the Poisson's ratio, which is an important parameter of elasticity, is kept constant at $\nu = 0.3$. We finally perform calculations to assess the effect of this parameter on the critical Ω values and on the distributions of the response variables. For this purpose we consider an FGM shaft with parameters $a/b = 0.5$ and $n = 0.4$. Note that calculations have already been performed for this shaft when $\nu = 0.3$. Here we study $\nu = 0.25$ and $\nu = 0.35$. The critical values of Ω obtained for different values of ν are given in Table 4.

As seen in Table 4, the elastic limits are affected notably by the change in the Poisson's ratio while the intermediate limits remain almost unaffected. Under $\Omega = 1.3$ we obtain the results given in Table 5. The corresponding distributions of the stress and displacement are plotted in Figure 9. The effect of ν can be visualized with the help of this figure.

Table 4. Limit angular speeds for different ν values.

Limits	$\nu = 0.25$	$\nu = 0.3$	$\nu = 0.35$
Ω_e	1.1403	1.1273	1.1128
Ω_2	1.2326	1.2434	1.2545
$\overline{r}_1$ (at Ω_2)	0.5741	0.5973	0.6238
Ω_3	1.3111	1.3145	1.3170
Ω_4	1.3176	1.3182	1.3187
$\overline{r}_2$ (at Ω_4)	0.6731	0.6927	0.7132

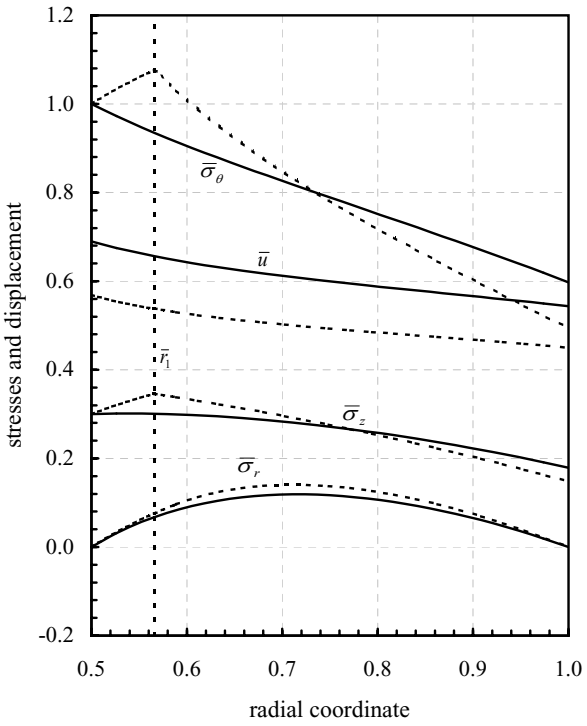

Figure 6. Stresses and displacement in the elastic stress state in an FGM shaft with fixed ends ($\epsilon_z = 0$) for $n = 0.6$ (solid lines) in comparison to those in a partially plastic homogeneous one (dashed lines) at $\Omega = 1.16481$.

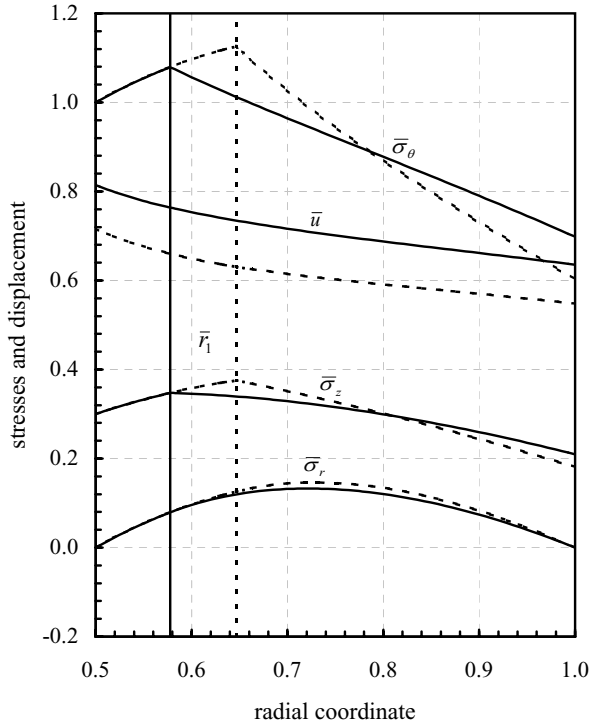

Figure 7. Stresses and displacement in the partially plastic stress state in an FGM shaft with fixed ends ($\epsilon_z = 0$) for $n = 0.6$ (solid lines) in comparison to those in a homogeneous one (dashed lines) at $\Omega = 1.25$.

Table 5. Calculated constants for $a/b = 0.5$ and $n = 0.4$ at $\Omega = 1.3$.

constants	$\nu = 0.25$	$\nu = 0.35$
$\overline{C}_3 \times 10^4$	8.98505	9.12899
$\overline{r}_1$	0.520884	0.556074
$\overline{C}_4$	0.904397	0.904397
$\overline{C}_5 \times 10^4$	9.63777	9.43778
$\overline{r}_2$	0.642234	0.678548
$\overline{C}_6 \times 10^4$	5.94244	7.00015
$\overline{C}_7 \times 10^2$	-1.09501	-1.23245
$\overline{r}_3$	0.782139	0.774996
$\overline{C}_1 \times 10^4$	4.36851	5.61716
$\overline{C}_2 \times 10^3$	1.42732	1.012497
$\overline{\epsilon}_z \times 10^4$	-6.19312	-8.42524

Concluding Remarks

Functionally graded materials (FGMs) have been widely used for the last 2 decades, particularly in high temperature and industrial (e.g., high speed cutting tools) applications, in microelectronics, and

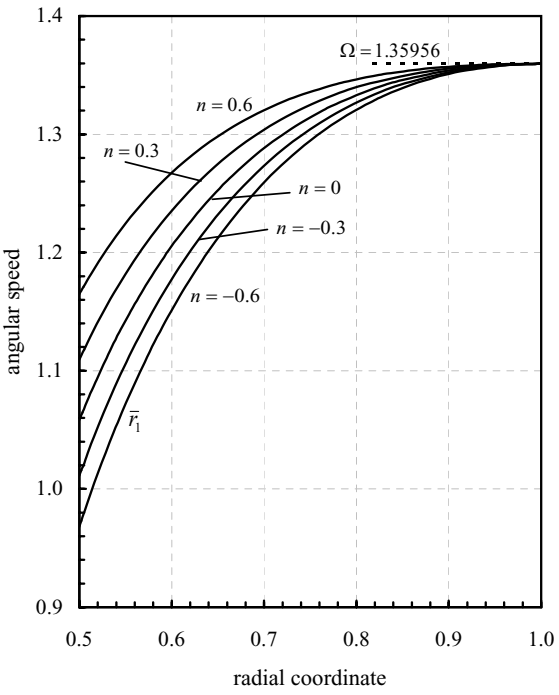

Figure 8. Expansion of plastically deformed region in FGM shafts with fixed ends ($\epsilon_z = 0$) for different n as Ω increases.

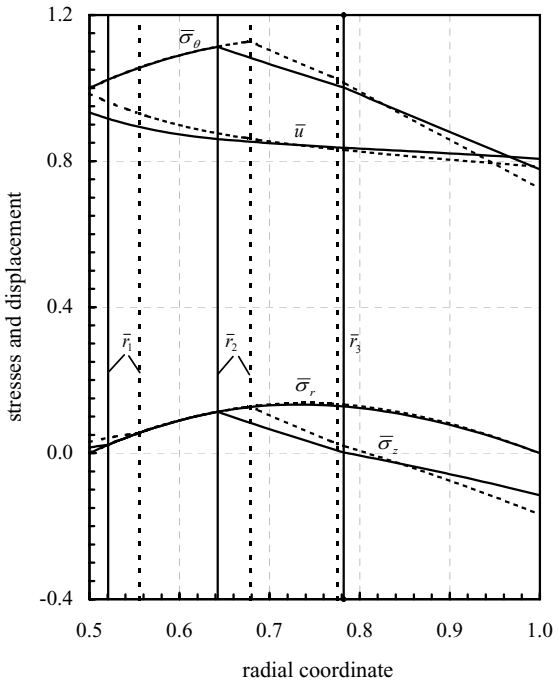

Figure 9. Stresses and displacement in the partially plastic stress state in an FGM shaft ($n = 0.4$) with free ends for $\nu = 0.25$ (solid lines) in comparison to those for $\nu = 0.35$ (dashed lines) at $\Omega = 1.3$.

in power transmission equipment. Among the various advantages of using FGMs, increasing strength, toughness, endurance limit, and resistance to corrosion, and retardation of the development of surface cracks are well known. In spite of these advantages, the stresses in rotating FGM shafts have not been well studied theoretically. There appears to be only one work in the literature (Eraslan and Akis, 2006) investigating the stresses and deformations in rotating FGM solid shafts. The modulus of elasticity of the shaft material was assumed to vary radially according to different nonlinear forms. Closed form solutions for rotating FGM solid shafts as well as solid disks both in the elastic stress state were derived. Another attempt is made here to proceed with studying the partially plastic stress state in rotating shafts. Calculations extending into the plastic range are important in engineering since the results allow one to have an idea about the level of residual stresses, which are generally used with advantage.

In the present work, specifically, generalized plane strain, $\epsilon_z = constant$, and plane strain, $\epsilon_z = 0$, analytical solutions for rotating partially plastic FGM hollow shafts are derived by considering variable modulus of elasticity. The plastic analysis is simply based on Tresca's yield criterion, its associated flow rule, and ideally plastic behavior. It is known that Tresca's flow rule can give plastic strains that do not agree well with experimental observations, leading to conservative results in elastic-plastic design problems. However, a previous work (Eraslan, 2004) indicates that the results of Tresca's and von Mises' criteria agree perfectly in the predictions of the stress and displacement fields for rotating shafts. On the other hand, the use of Tresca's yield condition and its associated flow rule for the analysis of rotating shafts and in many other problems results in linear differential equations, permitting analytical treatment of the problem. Such analytical solutions facilitate analysis of limiting cases and provide benchmark results for sophisticated FEM codes.

The stress response of a rotating partially plastic FGM hollow shaft when its modulus of elasticity varies continuously can be evaluated in the results of this work. Improvements in both elastic and partially plastic performances are possible if the shaft is designed so that the modulus of elasticity increases in the radial direction. Elastic limit rotation speeds increase and the expansion of the plastic core into the shaft is retarded. Nevertheless, the fully plastic rotation speed seems to be unaffected by the material nonhomogeneity caused by the variation in modulus of elasticity within the shaft.

As a final remark it is noted that the construction of governing differential equations, for the elastic and plastic regions, their particular solutions and all of the algebraic simplifications in this work were obtained by the inclusive use of Mathematica V4.1. Without such a powerful symbolic engine, the completion of this work might have taken several more years.

Nomenclature

a, b	inner and outer radii of the shaft (dimensionless inner radius $\overline{a} = a/b$)
C_i	integration constant
E	variable modulus of elasticity (reference value E_0)
F_z	axial force
n	material parameter (Eq. (1))
r, θ, z	cylindrical polar coordinates (dimensionless radial coordinate $\overline{r} = r/b$)
u	radial displacement (dimensionless form $\overline{u} = uE_0/(b\sigma_0)$)
ν	Poisson's ratio
ρ	mass density
ω	angular velocity (dimensionless form $\Omega = \omega b\sqrt{\rho/\sigma_0}$)
ϵ_i	normal strain component in $i-$direction (normalized form $\overline{\epsilon}_i = \epsilon_i E_0/\sigma_0$)
σ_0	uniaxial yield limit of the material
σ_i	normal stress component in $i-$direction (dimensionless form $\overline{\sigma}_i = \sigma_i/\sigma_0$)

References

Eraslan, A.N., "On The Linearly Hardening Rotating Solid Shaft", European Journal of Mechanics A/Solids, 22, 295-307, 2002.

Eraslan, A.N., "Von Mises' Yield Criterion and Nonlinearly Hardening Rotating Shafts", Acta Mechanica, 168, 129-144, 2004.

Eraslan A.N. and Akis T., "On The Plane Strain and Plane Stress Solutions of Functionally Graded Rotating Solid Shaft and Solid Disk Problems", Acta Mechanica, 181, 43-63, 2006.

Eraslan, A.N. and Mack, W., "A Computational Procedure for Estimating Residual Stresses and Secondary Plastic Flow Limits in Nonlinearly Strain Hardening Rotating Shafts", Forschung Im Ingenieurwesen/Engineering Research, 69, 65-75, 2005.

Eslami, M.R., Babaei, M.H. and Poultangari, R., "Thermal and Mechanical Stresses in a Functionally Graded Thick Sphere", International Journal of Pressure Vessels and Piping, 82, 522-527, 2005.

Gamer, U. and Lance, R.H., "Stress Distribution in a Rotating Elastic-Plastic Tube", Acta Mechanica, 50, 1-8, 1983.

Gamer, U., Mack, W. and Varga, I., "Rotating Elastic-Plastic Solid Shaft with Fixed Ends", International Journal of Engineering Science, 35, 253-267, 1997.

Güven, U. and Baykara, C., "On Stress Distributions in Functionally Graded Isotropic Spheres Subjected to Internal Pressure", Mechanics Research Communications, 28, 277-281, 2001.

Horgan, C.O. and Chan, A.M., "The Pressurized Hollow Cylinder or Disk Problem for Functionally Graded Isotropic Linearly Elastic Materials", Journal of Elasticity, 55, 43-59, 1999.

Liew, K.M., Kitipornchai S., Zhang, X.Z. and Lim C.W., "Analysis of Thermal Stress Behavior of Functionally Graded Hollow Circular Cylinders", International Journal of Solids and Structures, 40, 2355-2380, 2003.

Lindner, T. and Mack, W., "Residual Stresses in an Elastic-Plastic Shaft with Fixed Ends After Previous Rotation", The journal of Applied Mathematics and Mechanics (ZAMM), 78, 75-86, 1998.

Mack, W., "Rotating Elastic-Plastic Tube with Free Ends", International Journal of Solids and Structures, 27, 1461-1476, 1991a.

Mack, W., "The Rotating Elastic-Plastic Solid Shaft with Free Ends", Technische Mechanik, 12, 119-124, 1991b.

Timoshenko, S. and Goodier, J. N., Theory of Elasticity 3rd ed., McGraw-Hill New York, 1970.

Tutuncu, N. and Ozturk, M., "Exact Solution for Stress in Functionally Graded Pressure Vessels", Composites part B 32, 683-686, 2001.

Zimmerman, R. W. and Lutz, M.P., "Thermal Stresses and Thermal Expansion in a Uniformly Heated Functionally Graded Cylinder", Journal of Thermal Stresses, 22, 177-188, 1999.